Journal of Plant Biochemistry & Physiology
ISSN: 2329-9029

Zhu et al., J Plant Biochem Physiol 2015, 3:4
DOI: 10.4172/2329-9029.1000156

Research Article Open Access

If Photoinhibition of Soybean Photosystem II Enhances the Hypersensitive Response, It is Not Solely Due to Blockage of Electron Transfer Flow at D1

Jin Zhu[1], David J Neece[2], Bernarda Calla[1] and Steven J Clough[1,2]*

[1]*Department of Crop Sciences, University of Illinois, Urbana, IL, USA*
[2]*Agricultural Research Services, United States Department of Agriculture, Urbana, IL, USA*

Abstract

Previous studies have suggested that photoinhibition, through inactivation of photosystem II (PSII), could be beneficial to plants during defense to pathogens through enhanced reactive oxygen production, especially during the hypersensitive response (HR). In this study, we addressed this question by focusing on a possible role of turnover and inhibition of the PSII subunit D1, in defense to the compatible and incompatible strains of the bacterial pathogen *Pseudomonas syringae* in soybean leaves. Expression of the D1 encoding gene, *psbA*, as well as 14 other chloroplast encoded genes, was down regulated in response to *P. syringae*. This down regulation is consistent with reduced production of PSII components leading to increased photoinhibition of existing photocenters, and is also consistent with multiple studies showing a concerted down regulation of nuclear-encoded chloroplast genes during pathogen attack. However, although expression of the *psbA* transcript was reduced in response to pathogen within 8 hours of inoculation, the level of the *psbA* product, the D1 protein, showed no significant changes via western blots, and did not show any signs of degradation. Additionally, infiltrating leaves with the D1 inhibiting herbicide bentazon (competitive inhibitor of Q_B binding to D1, stopping photosynthesis by blocking electron transfer from Q_A to Q_B) together with *P. syringae* inoculation, showed that D1 inhibition did not enhance defense as expected (if photoinhibition enhanced defense), but actually rendered the host slightly more susceptible. The results reflect two possibilities. One is that PSII inhibition by blockage of electron flow through D1 of PSII, does not enhance resistance to *P. syringae*. The second possibility supported by the data is that the mechanism of photoinhibition during pathogen defense is not due solely to the blockage of electron flow, but through other means of stimulating photoinhibition, such as an inefficient degradation, removal, and replacement of damaged D1 from the PSII complex.

Keywords: Plant defense; Bacteria; Atrazine; Oxidative burst

Introduction

Under natural outdoor growing conditions, light levels are constantly fluctuating day-to-day, and hour-by-hour. Plants need to have mechanisms to deal with these constant changes. For example, when plants are exposed to excess light that surpasses the ability of the photosystems to utilize the absorbed energy, the photo protective mechanisms such as non-photochemical quenching, the water-water cycle, and photorespiration come into play to prevent damage [1,2]. However, often these protective measures are not sufficient to protect plant tissue from the excess light, resulting in light-induced photoinhibition which leads to production of reaction oxygen species (ROS) at damage proteins, membranes, and other cellular components [1-3]. The primary target of photodamage is the photosystem II multi-protein complex (PSII), of which D1 is the main component affected. As D1 is highly labile, it is continually damaged throughout the day, and therefore must be constantly replaced through subsequent degradation, removal, and *de novo* synthesis to maintain a functional PSII, and minimize damaging levels of ROS. Much of the repair occurs during the night, resetting PSII to be back to full functional capacity by the next morning.

The recent review by Nath et al. [4] details the complex processes that are believed to take place in the repair of photodamaged PSII and D1 subunit, involving cooperation from multiple chloroplast proteases [5]. Evidence suggests that damaged PSII is first phosphorylated, and that this phosphorylation leads the damaged PSII to leave the grana stacks and migrate into the stroma lamellae, where PSII it subsequently dephosphoryated and partially disassembled prior to the D1 subunit being acted upon sequentially by a several *FtsH* and Deg proteases. After breaking the 32 kDa D1 protein into 9 and 23 kDa peptides, it is replaced by *de novo* translation of the *psbA* transcript, which encodes D1. ROS, such as singlet oxygen, superoxide, and hydrogen peroxide, are believed do the initial damage to D1, and paradoxically, ROS have also been proposed to inhibit the *de novo* synthesis of the D1 protein at the translation step [6-8].

Studies in our lab and others have suggested a possible beneficial role for D1 lability in biotic stresses. Plant defense against pathogens and photoinhibition was measurable as a decrease in PSII operating efficiency in soybean within 8 hours of being inoculated with HR-inducing *Pseudomonas syringae* [9]. Research focused on a D1 degrading *FtsH* protease and disease resistance in tobacco, supports the possible link between levels of D1 protein and defense [10]. An *FtsH* gene homolog was found to display deceased transcription levels before the appearance of necrotic lesions in the HR induced by Tobacco Mosaic Virus (TMV) in tobacco. Furthermore, transgenic tobacco with an over-expressed *FtsH* was more susceptible to TMV, whereas transgenic tobacco with reduced *FtsH* expression was more resistant to the disease. It was also found that a nuclear-encoded *FtsH* gene was reduced at the transcript level in soybeans undergoing HR [9]. The accumulated evidence supports that decreased amounts

***Corresponding author:** Steven J. Clough, National Soybean Research Center, Department of Crop Sciences, University of Illinois, 1101 W. Peabody Drive, Urbana, IL 61801, USA, Tel: (217) 265-6452; E-mail: steven.clough@ars.usda.gov

Received September 30, 2015; **Accepted** October 26, 2015; **Published** November 02, 2015

Citation: Zhu J, Neece DJ, Calla B, Clough CJ (2015) If Photoinhibition of Soybean Photosystem II Enhances the Hypersensitive Response, It is Not Solely Due to Blockage of Electron Transfer Flow at D1. J Plant Biochem Physiol 3: 156. doi:10.4172/2329-9029.1000156

of *FtsH* expression interrupts the repair cycle of D1, increasing inactivation of PSII and inhibition of photosynthetic electron transfer, leading to reduced overall photosynthesis performance and increased ROS. Increased levels of ROS is well-known to provoke an accelerated defense responses and enhanced restriction of pathogen growth, and an enhanced ROS burst is present during the HR response to incompatible pathogen isolates, but absent in compatible interactions [11,12]. Speculation that the D1 protein may be affected by pathogen infection directly or indirectly, has also been heightened by the results of several studies showing that secreted pathogen effectors can enter the chloroplast and/or interact with chloroplast components [13,14].

In this study, we were interested in several aspects of D1 under disease stress: the transcript level, the total protein level, and the effect of a D1-interferring herbicide on soybean response to a compatible (virulent) and incompatible (avirulent) strains of *P. syringae*. This study addresses three hypotheses. Firstly, the *de novo* biosynthesis of D1 protein may be reduced during the HR, enhancing generation of the HR associated oxidative burst. Secondly, the total amount of D1 in HR samples would decrease, enhancing generation of the HR associated oxidative burst. Thirdly, a D1 interfering herbicide would enhance disease resistance by increasing the generation of an oxidative burst.

Materials and Methods

Plant material, inoculation and chlorophyll measurements

Soybean [*Glycine max* (L.) Merrill cv Williams 82, RPG1 dominant] plants were grown in a chamber at 22°C under a 16 hour light cycle with approximate light intensity of 200-250 µmol photons/m^2/sec as measured by a LI-COR (Lincoln, NE, USA) light meter (LI-250) and quantum sensor (LI-190SA). Fully developed unifoliate leaves were vacuum infiltrated as described [9]. Poorly infiltrated leaves were tagged and not used. Plants were placed back in the growth chamber immediately after infiltration. Bacterial inocula consisted of the strain *P. syringae* pv. *glycinea* Race 4 with or without the avirulence gene *avrB* at a concentration of approximately 2×10^7 colony-forming units (CFU) ml^{-1} in water. Control leaves were infiltrated with water. For D1 and transcript level assays, infiltrated plants were collected at 2, 8 and 24 hours post inoculation (hpi) or 2, 4, 8 hours hpi. In the study on the effect of bentazon on defense against this bacterial pathogen, sodium bentazon (a generous gift from BASF) was dissolved into the bacterial suspension (2×10^5 CFU ml^{-1}) and the control (no bacteria). Chlorophyll fluorescence was measured using a Walz Imaging PAM (Walz GmbH, Effeltrich, Germany) and the maximum quantum efficiency of PSII (Fv/Fm) was determined as previously described [9].

Transcript expression of chloroplast encoded genes

Total RNA was extracted and cleaned as described [9]. Random hexamer primers (Invitrogen, CA, USA) were used to prime the synthesis of cDNA from total RNA. Firstly, 3 µg total clean RNA was incubated with DNase I (Invitrogen, CA, USA) in a total 10 µl reaction at room temperature for 15 minutes to remove DNA, followed by incubation at 65 °C for 10 min to inactivate DNase I. Secondly, the DNA-free RNA was incubated with random hexamers and dNTPs (Bioline, MA, USA) at 65°C for 5 min, then chilled on ice for at least 1 minute. The reaction was subjected to reverse transcription using Superscript II First-Strand Synthesis System for RT-PCR (Invitrogen, CA, USA) according to the manufacturer's instructions. The RNA was removed from synthesized cDNA using RNase H (Invitrogen, CA, USA). The following qRT-PCR was conducted essentially as described previously [15]. The primers for the target gene (Supplemental Table 1) were designed based on the chloroplast gene sequences obtained from NCBI (http://www.ncbi.nlm.nih.gov/entrez/viewer.fcgi?db=nucleotide&val=83595723) using Primer 3.0 software [16]. The expression of a soybean β-actin gene (GenBank XM_003531518.2) was used as the internal standard to normalize the small difference in template amounts. The qRT-PCR data were analyzed using the relative quantification $2^{-\Delta\Delta CT}$ method (Livak and Schmittgen, 2001) and fold change was transformed into $\log_2$ ratio. Three biological and two technical replicates were conducted on every comparison between treatment and control. Standard error was calculated based on the three biological replicates.

Thylakoid membrane protein isolation

Soybean thylakoid membrane proteins were isolated essentially as described previously [17]. Unifoliate leaves from six plants (12 leaves total) were de-veined with a straight-edged razor, and pooled before being homogenized in a Warning Blender at high speed for 30 s in 100 ml grinding buffer containing 50 mm MES-KOH (Sigma, MO, USA) (pH 6.5), 0.3 M NaCl (Fisher Scientific, PA, USA), 10 mm KCI (Fisher Scientific, PA, USA), 2 mm EDTA (Fisher Scientific, PA, USA), 1 mm EGTA (Sigma, MO, USA), 0.2% (w/v) fatty-acid-free BSA (Sigma, MO, USA), and 10 mM ascorbate (Sigma, MO, USA). The homogenate was then filtered through 16 layers of cheesecloth, and the filtrate was centrifuged for 2 min at 2400 × *g*. The resulting pellet was suspended with a soft paintbrush in 15 ml of a low osmotic strength buffer containing 5 mM MES-KOH (pH 6.5), 50 mM sorbitol, 10 mM KCl, 2 mM $MgCl_2$, 1 mM EGTA, and 10 mM ascorbate to promote the removal of adhering stromal proteins. The sample was centrifuged for 15 s and then filtered through a Kimwipe immobilized on a 50 ml tube with a rubber band. The filtrate was then centrifuged for 4 min at 2500 × *g*. The pellet was suspended in the same low osmotic medium and centrifuged for 4 min at 2500 × *g*. The final thylakoid pellet was suspended in 0.5 mL of a solution containing 5 mM MES-KOH (pH 6.5), 0.4 M sorbitol, 10 mM KCl, 2 mM $MgCl_2$, 1 mM EGTA, and 10 mM ascorbate. All manipulations were performed at approximately 4°C. The thylakoid extracts were stored at -80°C until they were solubilized for polypeptide analysis.

Protein quantification

Bradford reagent (Sigma, MO, USA) was used to quantify total protein following a 96-well plate assay protocol. Protein standards were prepared with BSA with a range from 0-1.0 mg/ml with the protein buffer containing 5 mM MES-KOH (pH 6.5), 0.4 M sorbitol, 10 mM KCl, 2 mM $MgCl_2$, 1 mM EGTA, and 10 mM ascorbate. Sample proteins were diluted at 1:10 with the protein buffer. Five microliters of each sample or BSA standard was mixed with 250 µl Bradford reagent followed by incubation at room temperature for 15 minutes. The plates were read using a BioTek Microplate Reader (BioTek Instruments, Vermont, USA) and the endpoint data of absorbance at A_{595} was collected and analyzed with Gen 5.0 software (BioTek Instruments, VT, USA).

SDS-PAGE and gel transfer

Protein separation by SDS-PAGE was performed essentially as described previously [18]. Equal amounts of thylakoid membrane protein samples were mixed with Laemmilli sample buffer (Bio-rad, CA, USA) with beta-mecaptoethanol (Sigma, MO, USA) at 1:1 ratio and heated at 70°C for 10 minutes prior to running on a 10-20% gradient SDS-PAGE Ready Gel (Bio-rad, CA, USA) in a Mini-PROTEAN 3 Cell vertical electrophoresis apparatus (Bio-rad, CA, USA). Ten µg protein samples were equally loaded (Supplemental Figure 1). Kaleidoscope pre-stained protein standards (Bio-Rad, CA, USA) were used to

estimate molecular weights. Samples were run in SDS-PAGE for 35 minutes at 200 volts before electro-blotted onto an Immobilon-P PVDF membrane (Millipore, MA, USA) in a Mini Tank using a Bio-Rad Transblot Cell (Bio-Rad, CA, USA) operated at constant current (200 mA) for 3 h with cooling according to manufacturer protocol.

Western blotting

Electro-blotted PVDF membrane was blocked with 8% BSA (Sigma, MO, USA) with agitation at 4°C overnight, followed by incubation with primary antibody (1:5000) for 1.5 h. Polyclonal D1 antibodies were designed and raised against a synthetic oligopeptides produced by Gene Script, NJ, USA. Titration experiment with serial 2-fold dilutions of proteins was conducted and 10 µg protein was determined as the ideal input amount for western blotting (Supplemental Figure 2). PVDF membrane was washed five minutes thrice with TTBS buffer (Tris-buffered saline with 0.05% Tween-20 (Sigma, MO, USA) and then incubated with secondary antibody, conjugated alkaline phosphatase (Sigma, MO, USA), diluted 1:100,000. The immunodetection was obtained by using BCIP/NBT liquid substrate system (Sigma, MO, USA).

Total phenolic assay

Total phenolic assay was performed as described in publications [18]. Basically, the equal length of main vein from leaf sample of similar size was collected and stored at -80°C. Frozen tissue was moved into a 2 ml screw cap tube with 0.75 ml 95% methanol and three tungsten carbide beads. The tissue was homogenized in a tissue shredder (Qiagen, CA, USA) for 5 min at 30 Hz and incubated at room temperature in the dark for 48 h after tungsten beads were removed. After incubation, the extraction was centrifuge for 5 min at 13,000 × *g* and supernatant was transferred to a 1.5 ml microfuge tube. For each sample, 125 µl was pipetted into a new tube. Two tubes were made for technical replicates. 250 µl of 10% F-C reagent (Sigma, MO, USA) was added into each tube. After mixing, 1 ml of 700 mM Na_2CO_3 (Fisher Scientific, PA, USA) was added into solution and mixed again. Gallic acid (Sigma, MO, USA) standards from 31.5 µM to 10 mM were created and treated with F-C reagent and Na_2CO_3 in the same manner as sample treatment. All tubes, including samples and gallic acid standards, were placed in the dark at room temperature for 2 h. After incubation, 150 µl from each tube was added into 96 well plates and the plates were read for end-point absorbance at 750 nm with a BioTek plate reader (BioTek, CA, USA). To analyze the results, a standard curve was calculated from the blank-corrected A_{765} reading of the gallic acid standards. The total phenolics as gallic acid equivalents were calculated using the regression equation between gallic acid standards and A_{765} absorbance.

Quantitative measurement of bacterial multiplication in soybean leaves

A single leaf disc of 1 cm^2 from each treated sample was collected and ground thoroughly in 200 µl sterile nanopure H_2O. The homogenous solution was diluted at 1:10 in series until 1:10,000. Ten µl of diluted solution of each concentration was plated followed by incubation at 28 °C for 1-2 days until countable colonies formed. The numbers of colonies were recorded for each dilution and average number of colonies was calculated. Finally, the average colony number per disc from every treatment was calculated and standard error was derived from four biological replicates.

Results

Effect of *P. syringae* compatible and incompatible infection on expression of chloroplast encoded genes

Fifteen chloroplast genes were chosen for qRT-PCR analysis to monitor their transcript level in soybean during both the incompatible and compatible interactions induced by *P. syringae* at 2, 4 and 8 hpi. The 15 genes were representatives of important components involved in photosynthetic electron transportation and ATP synthesis in photosystems, including the gene encoding PSII subunit D1, *psbA*. Generally, all the 15 genes decreased at all-time points, had up to a 2-fold reduction in the compatible interaction, and up to a 5-fold reduction in the incompatible interactions, compared to uninoculated controls (Figure 1). The amplitude of transcript suppression increased with time and peaked at T8, and the differential expression changes were more dramatic in the incompatible interaction (HR) than in the compatible interaction for all genes tested.

Although chloroplast transcripts are highly abundant, we could detect expression changes using qRT-PCR. The great abundance of chloroplast RNA was reflected in our qRT-PCR study, as the Ct values were as low as 15 while most genomic genes have Cts around 25 or more. The chloroplast genes encoding the D1 and D2 subunits of PSII (*psbA* and *psbD*, respectively) decreased across all time points in both compatible and incompatible reactions and the $\log_2$ transformed fold changes reached the highest at 8 hpi, with -2.8 and -2.26 respectively in incompatible, but only -0.56 and -0.23 in compatible interaction. Similar modulation occurred for the other three PSII components monitored: *psbC* encoding CP43 chlorophyll binding apoprotein, *psbH* encoding phosphoreprotein, *psbZ* encoding small protein Z, and *psbK* encoding small protein K; all showing a greater reduction in HR. Other chloroplast encoded genes investigated included: *psaA* and *psaB* encoding the reaction center proteins for PSI, PSI assembly protein Ycf3, two genes encoding ATP synthase subunits, cytochrome b6 and cytochrome f, cytochrome b6/f complex subunit IV and large RUBISCO subunit. The transcript expression levels of all these genes displayed similar down-regulated trends as the PSII associated genes, with the greatest reduction at 8 hpi during the incompatible HR interaction.

D1 protein level dynamics during pathogen infection

Antibodies to D1 were raised to determine the level of this protein by western blotting. We visually analyzed published predicted folding models for the D1 protein (Supplemental Figure 1) and identified two exposed regions that were predicted to be antigenic. Synthetic peptides from these regions were used to produce antibody 'A' to the AB loop (PVDIDGIREPVSG) near the N-terminus, and antibody 'B' to the DE loop (RETTENESANEGYRFGQEEE) near the C-terminus. Regardless of antibody used, western blots revealed similar detection capabilities; therefore antibody 'A' was chosen for use in the assays presented. A BLASTp search for possible cross reacting proteins to antibody 'A', hit only D1 with 100% identity to PVDIDGIREPVSG, and hit multiple other proteins matching between six to 10 of the 13 residues Although this antibody produced two bands on the western blot, we believe both are the intact form of D1, and not cross hybridization, as previous researchers have shown that it is common to see two bands for intact D1 [19,20]. Moreover, if the lower band is cut out and re-ran, both bands appear again on the new gel, indicating that the lower band is a conformer of the intact 32 kDa protein [19].

Western blotting was performed to monitor the total D1 protein accumulation from thylakoids. Thylakoid membrane proteins were

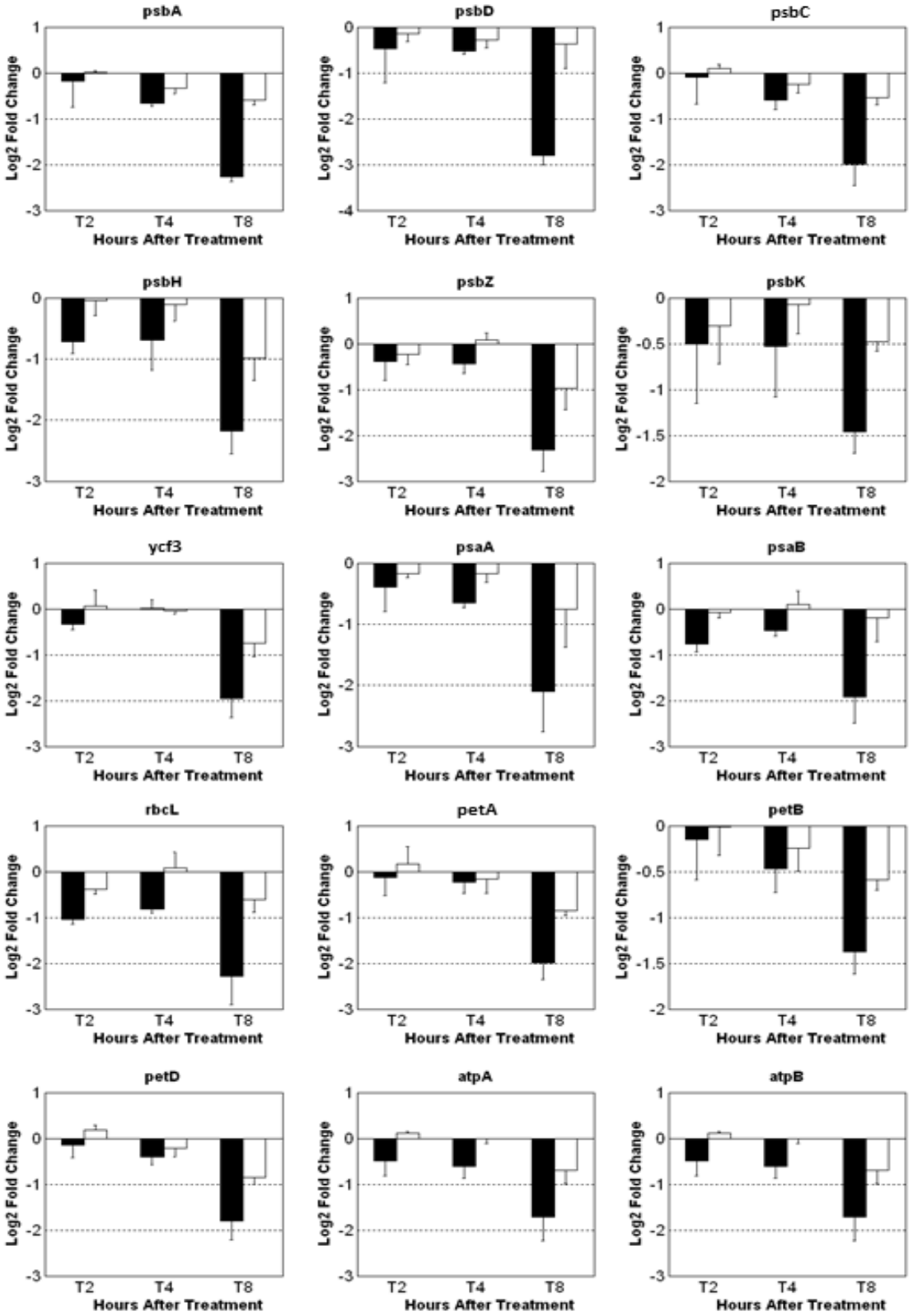

Figure 1: Chloroplast gene expression data measured by qRT-PCR. Open and closed bars represent compatible and incompatible interactions provoked by virulent and avirulent bacteria respectively. Expression levels are given as $\log_2$ transformed fold change, inoculated samples versus uninoculated controls. QRT-PCR data represent the average values obtained from three independent biological replicates. Error bars represent the standard errors of the three replicates.

extracted from soybean leaves and quantified. The titration experiments determined that loading 10 µg protein was suitable for later immune detection of any decreases in abundance (Supplemental Figure 2). Equal quantity of thylakoid membrane proteins from each sample was assayed by SDS-PAGE (Supplemental Figure 3). The resulting gel was blotted to PVDF membrane followed by membrane hybridization and colometric assay. The western blotting did not reveal any significant difference in the expression level of D1 protein between treatment and control (Figure 2). The western blot also did not reveal any obvious degradation products, and only the approximate 32 kDa band (and its faster migrating conformer) is apparent for all treatments and control, and all time points.

The effect of enhanced PSII inhibition on defense response to P. syringae

To directly test if PSII inhibition caused by the disruption of electron transfer flow affects defense to pathogens, the D1 interfering herbicide bentazon (competitive inhibitor of Q_B binding to D1) was used. To find a concentration of bentazon that would inhibit PSII enough to be measurable, but not likely to kill the host tissue, 0.3, 0.8, and 1.2 mM bentazon was vacuum infiltrated into soybean leaves, and photoinhibition was monitored by measuring PSII efficiency by determining fluorescence levels related to Fv/Fm at 2, 4, and 8 hours post infiltration (Figure 3). Bentazon at the concentration of 0.3 mM showed no measurable effect on PSII inhibition, whereas 1.2 mM bentazon had a too strong of an effect that continued during the 8 hour time course. Infiltration of 0.8 mM bentazon gave the transient response desired, as it reduced PSII efficiency by nearly 70% by 2 hpt, and then the leaf tissue fully recovered by 8 hpt (soybean are able to detoxify bentazon). The 0.8 mM levels measurably inhibited PSII for at least 4 hours, and did not lead to any visible damage to plants, as no chlorosis or necrosis appeared after treatment (Supplemental Figure 4 and 5). Additionally, when testing if bentazon had any direct toxic effect on growth of the pathogen in culture, incubation of *P. syringae* in liquid medium in the presence of 0.8 mM bentazon had little to no effect on the growth of the bacterial cultures as determined by optical density of overnight cultures that started at the same cell density (OD_{600}=0.26 for avirulent bacteria, OD_{600}=0.27 for avirulent bacteria with 0.8 mM bentazon, and OD_{600}=0.22 for virulent bacteria and OD_{600}=0.21 for virulent bacteria with 0.8 mM bentazon). Therefore, experiments to study effects of co-infiltration of *P. syringae* and the D1-interfering herbicide, utilized bentazon at 0.8 mM.

To determine if inhibition of electron flow at D1 would relieve or aggravate disease resistance to *P. syringae*, we took visual observations of the chlorosis and necrosis development in leaf tissue during the first 48 hours after co-infiltration with bentazon. No visible chlorosis or necrosis was observed in leaves treated with virulent strain of the pathogen of 2×10^7 CFU ml^{-1}, nor with straight 0.8 mM bentazon at 24 hpi; however, co-infiltration of bentazon and the virulent pathogen together led to significant formation of chlorosis, and necrosis (Supplemental Figure 4). The chlorosis and necrosis was also seen in leaves treated with the avirulent pathogen, but addition of bentazon did not cause any apparent additive effect on lesion development (Supplemental Figure 5). However, addition of bentazon did cause accumulation of large patches of dark pigment forming along the main veins of leaves (Supplemental Figure 5) and this effect was not seen in leaves treated with virulent pathogen (Supplemental Figure 4).

We suspected that the dark pigment along main veins in leaves treated with bentazon and the incompatible *P. syringae* carrying *avrB*, was due to phenolic production, as phenolics are known to be produced in leaf epidermis to absorb UV light under high-light stress. Therefore, total phenolic assays were conducted to investigate phenolic accumulation in the main veins of leaves treated with bentazon or bacteria, or a combination of both. In order to be consistent with the bacterial growth study, a lower concentration (2×10^5 CFU ml^{-1}) of bacteria was used for infection. The results (Figure 4) showed: (1) by 24 hpt, total phenolic content in the leaves from different treatments were similar and did not change over time; (2) by 48 hpt, total phenolic content in leaves infiltrated with bentazon or compatible *P. syringae* or combination of both, remained the same; (3) by 48 hpt, total phenolic content in leaves infiltrated with incompatible *P. syringae,* or a combination of bentazon and this strain, was significantly increased; (4) by 48 hpt, total phenolic content in leaves infiltrated with a combination of bentazon and incompatible *P. syringae* was significantly higher than in leaves infiltrated with incompatible bacteria only.

Addition of 0.8 mM bentazon to induce PSII inhibition in a *P. syringae* inoculation, enhanced disease symptoms induced by the virulent bacterial strain, and enhanced phenolic production when added to an incompatible strain. But the question remained as to whether or not the symptoms were due to enhanced defense, or enhanced virulence. To determine the difference, and to directly test if inhibition of electron transfer through PSII could enhance defense, we conducted bacterial growth experiments to examine the effect of bentazon on bacterial multiplication within soybean leaves. The bacterial growth curves (Figure 5) displayed: (1) as expected, bacteria growth in leaves infiltrated with incompatible *P. syringae* carrying *avrB*,

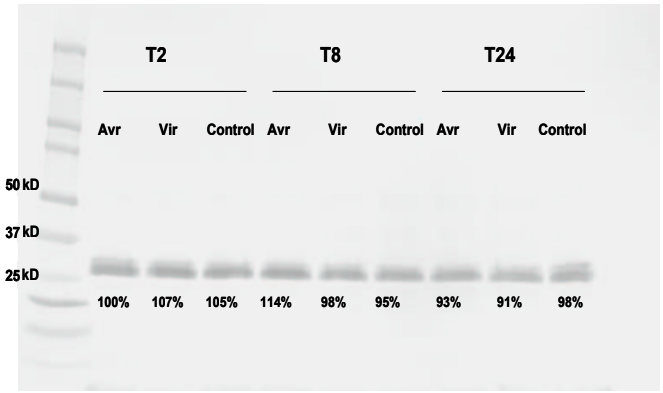

Figure 2: Western blot analysis of D1 protein abundance in soybean leaves infiltrated with *P. syringae*. Avr: *P. syringae* with *avrB* gene. Vir: *P. syringae* without *avrB* gene. Control: water. The signal of bands was quantified with Matlab.

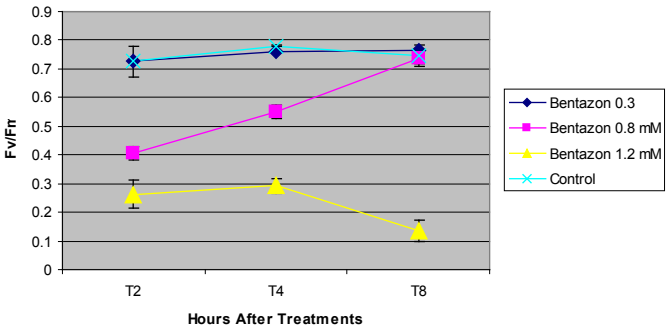

Figure 3: Chlorophyll fluorescence measurement of leaves infiltrated with different concentrations of bentazon and water as control. The value is the average of five replicates and the error bar represents standard error.

bacterial multiplication was lower than in leaves infiltrated with the compatible strain (lacks *avrB*) across the time course; (2) surprisingly, bentazon imposed a beneficial effect on bacterial multiplication in leaves infiltrated with compatible strain across the time course; (3) by day 3, bentazon imposed a beneficial effect on bacterial multiplication in leaves infiltrated with incompatible bacteria as well.

Discussion

Although ROS can be generated by numerous reactions and from different sources within a plant [21], recent evidence has been accumulating in support of a possible connection between photosynthesis inactivation, ROS and defense response, specifically, that photoinhibition is playing a role in the large secondary oxidative burst that is seen in the HR defense response. However, precise mechanisms linking these events are still obscure. In this report, several studies were conducted to determine if enhanced D1 degradation, and/or the reduction of electron flow through D1, aides in defense to *P. syringae*.

A general reduction of nearly 100 nuclear-encoded photosynthetic-related genes was reported to occur within 8 hpi, which is prior to symptom development [9]. Additionally, chlorophyll fluorescence measurements of soybean leaves undergoing HR revealed a reduction of ΦPSII and Fv/Fm, indicating reduced maximum quantum yield of photosynthetic electron transport and inhibition of the PSII reaction center in the absence of necrosis in the treated leaves at 8 hpi [9]. Others have also reported on reduced photosynthesis activity, especially photosynthetic electron transport, when plants were invaded by pathogens or attacked by insects [22,23]. The research on photoinhibition in plant cells treated with an HR elicitor [24], and the observed enhanced defense to viral infection in *ftsH* mutants [10], also hinted at a benefit to decreasing photosynthetic activity during plant defense. Based on these reports, and on the fact that D1 is very labile to oxidative stress, we hypothesized that plants might benefit by down regulating the expression and replacement of D1 (and resulting reduction in electron flow) as a means of rapidly enhancing ROS production through excess light energy that is unable to be properly dissipated through the photosystem centers. Such a mechanism would contribute to the ROS oxidative burst and enhance defense responses, in addition to reducing photosynthesis in the infected site yielding less sugar, which would also restrict the growth of invading pathogen.

Genes encoding the proteins that make up photosynthetic components of the chloroplast are split between chloroplast and nuclear locations, and this current study, in combination with our previous microarray study [9], revealed that both chloroplast and nuclear encoded photosynthesis genes, including the genes *phbA* (D1) and *ftsH*, tended to be down regulated in response to *P. syringae* infection. Although the gene expression analysis in this current study showed a down regulation of *psbA*, its gene product, D1, was shown to remain at a relatively stable level, and to not be degraded, in all the treatment and controls, as determined by western blotting. This discrepancy between transcript level and protein level has been noted before for other chloroplast genes, as differential expressed chloroplast proteins are mainly regulated at the posttranscriptional and translational level in mature chloroplasts [25].

In order to determine if there is a role for D1 in defense, a D1-interfering herbicide, bentazon, was utilized to inhibit D1 function, and plants subsequently monitored for changes in defense performance. Bentazon is in the benzothiadiazoles class of herbicides, and has the same mode of action as atrazine: competitive inhibition of quinone B (Q_B) binding to D1 [26]. The proper binding of Q_B to D1 is critical to the ability of Q_B to accept electrons from Q_A. The herbicides atrazine and bentazon block the ability of D1 to properly associate with Q_B, thereby nullifying electron transfer and PSII activity. In the presence of light and blocked electron transfer, oxidative damage is accelerated and cell death rapidly ensues.

Chlorophyll fluorescence measurements showed that the effect of 0.8 mM bentazon was to inhibit PSII by 70% during the initial 2 hours post infiltration, and to relax inhibition by 8 hours; hence the inhibitory effect on PSII was quick and transient under these experimental conditions. If an initial transient inhibition of PSII was an important factor for initiation of the ROS burst and HR, we would have expected enhanced resistance to both virulent and avirulent pathogen strains by inhibiting PSII 70% within 2 hpi. In contrast to this expectation, the application of bentazon had a slightly positive effect on pathogen population growth within the tissue (bentazon did not have an effect on bacterial growth in nutrient culture medium). While this result is not well understood, similar results have been reported, where treatment of another D1 inhibiting herbicide, DCMU, increased viral load in the infected leaves in tobacco with either dominant *NN* resistant or recessive *nn* genotypes [27]. There are a few possible explanations. Firstly, *P. syringae* requires partial stimulation of cell death pathways to establish disease [28]. Bentazon may slightly stimulate these cell death pathways to the point of helping the bacteria, but not to the point of accelerating defenses and restricting pathogen population growth. Secondly, photosynthesis inhibition caused by bentazon at a very early

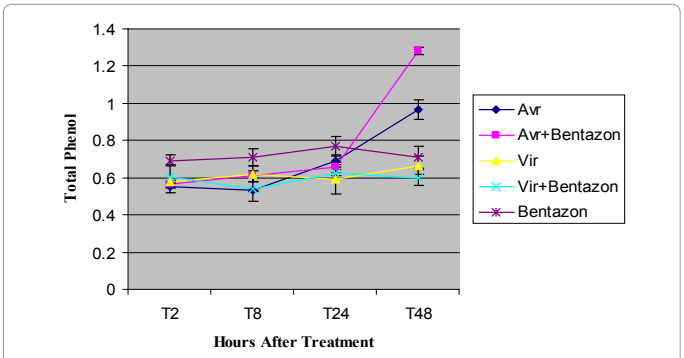

Figure 4: Total phenolic assay on leaves infiltrated with bentazon, bacteria, or bentazon and bacteria. The value is average of three replicates and the error bar represents standard error. Avr: *P. syringae* with *avrB* gene. Vir: *P. syringae* without *avrB* gene. Bacterial inoculum was at 2 × 10^5 CFU ml^{-1}

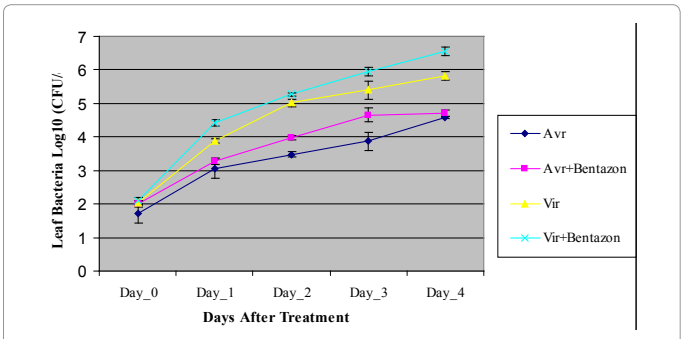

Figure 5: Bacterial growth on leaves infiltrated with bentazon or bacteria or both. The bacteria amount is calculated as total bacterial colonies per cm^2 and number is log_{10} transformed. The value is the average of three replicates and the error bar represents standard error. Avr: *P. syringae* with *avrB* gene. Vir: *P. syringae* without *avrB* gene. Control: Water. Bacterial inoculum was at 2 × 10^5 CFU ml^{-1}

time point might lead to decreased production of energy (ATP) and reducing power (NADPH) needed for rapid synthesis and activity of many new defense-related proteins. Thirdly, as many defense compounds are dependent on biochemical pathways in the chloroplast, Bentazon may have indirectly reduced defense-related molecular building blocks, such as those needed to feed the phenylpropanoid pathway [15,29], leading to compromised defense against pathogens. Fourthly, bentazon is found to inhibit expression of several apoptosis-related genes in soybean [15], which may slow impeded programmed cell death in leaves undergoing HR. Any of these effects would benefit bacterial multiplication since the robustness of the defense response has been shown to be key in providing resistance in the HR [9,30]. Another possible outcome of the addition of bentazon at the initial inoculation phase, especially for the incompatible interaction, was that a heightened production of ROS might have occurred as expected for this herbicide, but instead of enhancing the defense pathways, it might have instead heightened the production of antioxidants, such as the production of phenolics like hydroxycinnamic acids, flavonoids, anthocyanins, tannins and lignins. These phenolic compounds are considered to be strong antioxidants in plants and are often induced in tissue undergoing oxidative stress, especially in response to singlet oxygen and superoxide, both of which are produced in photoinhibition [4,31,32]. This possibility might explain why the total phenolics assay revealed that the leaves coinfiltrated with bentazon and the incompatible pathogen accumulated more phenolics than compatible pathogen infected leaves, and could explain why the plants endured greater pathogen numbers during the infection periods when bentazon was added to the inoculum, as the anti-oxidants could have dampened the effectiveness of the ROS to trigger maximal defenses. Therefore, bentazon treatment might have diverted phenolic substrates away from the phehylpropanoid pathway and the antimicrobial isoflavones, but instead towards other phenolics that might be more suited for UV absorption [15,29]. If this were to be the case, then the fact that bentazon alone did not impose a noticeable effect on phenolic accumulation, suggests that the phenolics production was primed by the herbicide, but only surpassed a threshold level needed to induce the high level of these anti-oxidants once the incompatible pathogen was also present in high enough numbers to activate the HR.

In summary, this study showed that *P. syringae* infection decreased transcript levels of *psbA* but did not affect steady state D1 protein levels. D1 interfering bentazon aggravated disease symptoms and benefited bacterial growth in leaves infected with virulent bacteria. Bentazon also benefited bacterial growth in leaves infected with avirulent bacteria but did not aggravate disease symptoms. Meanwhile, bentazon provoked more accumulation of phenolics along the main veins when co-infiltrated into leaves with avirulent bacteria.

Taken together, the studies do not clearly support the hypothesis that the plants enhance ROS production and the HR solely via blocking D1 function or enhanced degradation. However, the data is consistent with enhanced ROS being generated by a lack of D1 repair occurring during the HR (i.e., D1 could be continually damaged, but is not being degraded/removed/replaced). Future experiments that could enhance this study are needed. For one, *in vivo* pulse labeling would reveal more information about any *de novo* synthesis of D1 and degradation of D1 protein under stress. It would be informative to analyze global gene expression in soybean leaves coinfiltrated with both bentazon and *P. syringae* to ascertain possible explanation for the enhanced production of phenolics, and a chemical analysis of these phenolics to determine more precisely what classes of phenolics are being produced, as well as to possibly shine light as to why there is such a strong and rapid down regulation of transcription of so many photosynthesis genes hours after inoculation with an HR-inducing microbe. Additionally, as phosphorylation has been shown to be required for D1 turnover [4] it would be interesting to determine phosphorylation changes of PSII components during HR.

Acknowledgements

Authors would like to thank professors Don Ort and Lisa Ainsworth (both USDA-ARS at the University of Illinois campus) for assisting us with our understanding of photosynthesis. We also thank Osman Radwan for assisting with pipetting qRT-PCR plates when the lead author had a wrist injury. We thank Professor Steve Huber (USDA-ARS at the University of Illinois campus) for assistance in identification of the antigenic regions of D1, and he and Xia Wu for their advice on protein work. Finally, we would like to thank the main funding sources: USDA-ARS (the base CRIS funding to SJC) and a grant from University of Illinois Soybean Disease Biotechnology Center to SJC. Mention of trade names or commercial products in this publication is solely for the purpose of providing specific information and does not imply recommendation or endorsement by the U.S. Department of Agriculture.

References

1. Apel K, Hirt H (2004) Reactive oxygen species: metabolism, oxidative stress, and signal transduction. Annual Review of Plant Biology 55: 373-399.
2. Ort DR (2001) When there is too much light. Plant Physiology 125: 29-32.
3. Asada K (2000) The water-water cycle as alternative photon and electron sinks. Philosophical Transactions of the Royal Society B: Biological Sciences 355: 1419-1431.
4. Nath K, Jajoo A, Poudyal RS, Timilsina R, Park YS, et.al. (2013) towards a critical understanding of the photosystem II repair mechanism and its regulation during stress conditions. FEBS Letters 587: 3372-3381.
5. Kato Y, Sun X, Zhang L, Sakamoto W (2012) Cooperative D1 degradation in the photosystem II repair mediated by chloroplastic proteases in Arabidopsis. Plant Physiology 159: 1428-1439.
6. Nishiyama Y, Allakhverdiev SI, Murata N (2011) Protein synthesis is the primary target of reactive oxygen species in the photoinhibition of photosystem II. Physiologia Plantarum 142, 35-46.
7. Nishiyama Y, Allakhverdiev SI, Yamamoto H, Hayashi H, Murata N (2004) Singlet oxygen inhibits the repair of photosystem II by suppressing the translation elongation of the D1 protein in *Synechocystis sp. PCC 6803*. Biochemistry 43: 11321-11330.
8. Nishiyama Y, Yamamoto H, Allakhverdiev SI, Inaba M, Yokota A, et al. (2001) Oxidative stress inhibits the repair of photodamage to the photosynthetic machinery. The EMBO Journal 20: 5587-5594.
9. Zou J, Rodriguez-Zas S, Aldea M, Li M, Zhu J, et al. (2005) Expression profiling soybean response to *Pseudomonas syringae* reveals new defense-related genes and rapid HR-specific down regulation of photosynthesis. Molecular Plant-Microbe Interactions 18: 1161-1174.
10. Seo S, Okamoto M, Iwai T, Iwano M, Fukui K, et al. (2000) Reduced levels of chloroplast FtsH protein in tobacco mosaic virus-infected tobacco leaves accelerate the hypersensitive reaction. The Plant Cell 12: 917-932.
11. Doke N, Miura Y, Sanchez LM, Park HJ, Noritake T, et al. (1996) The oxidative burst protects plants against pathogen attack: mechanism and role as an emergency signal for plant bio-defence - a review. Gene 179: 45-51.
12. Doke N, Ohashi Y (1988) Involvement of an O2- generating system in the induction of necrotic lesions on tobacco leaves infected with tobacco mosaic virus. Physiological and Molecular Plant *Pathololgy* 32: 163-175.
13. Guttman DS, Vinatzer BA, Sarkar SF, Ranall MV, Kettler G, et al. (2002) A functional screen for the type III (Hrp) secretome of the plant pathogen *Pseudomonas syringae*. Science 295: 1722-1726.
14. Jelenska J, Yao N, Vinatzer BA, Wright CM, Brodsky JL, et al. (2007) AJ domain virulence effector of *Pseudomonas syringae* remodels host chloroplasts and suppresses defenses. Current Biology 17: 499-508.
15. Zhu J, Patzoldt WL, Radwan O, Tranel PJ, Clough SJ (2009) Effects of photosystem-II-interfering herbicides atrazine and bentazon on the soybean transcriptome. Plant Genome 2: 101-205.
16. Rozen S, Skaletsky HJ, Krawetz S, Misener S (2000) Bioinformatics methods and protocols: methods in molecular biology. Humana Press, Totowa, NJ.

17. Ainsworth EA, Gillespie KM (2007) Estimation of total phenolic content and other oxidation substrates in plant tissues using Folin-Ciocalteu reagent. Nature Protocols 2: 875-877.

18. Cooper P, Ort DR (1988) Changes in protein synthesis induced in tomato by chilling. Plant Physiology 88: 454-461.

19. Greenburg BM, Gab V, Mattoo AK, Edelman M (1987) Identification of a primary in vivo degradation product of the rapidly-turning-over 32 kd protein of photosystem II. EMBO J. 6: 2865-2869.

20. Kettunen R, Tyystjarvi E, Aro EM (1996) Cool Degradation pattern of photosystem II reaction center protein D1 in intact leaves. Plant Physiology 111: 1183-1190.

21. Tripathy BC, Oelmüller R (2012) Reactive oxygen species generation and signaling in plants. Plant Signaling & Behavior 7: 1621-1633.

22. Rahoutei J, Garcia-Luque I, Baron M (2000) Inhibition of photosynthesis by viral infection: effect on PSII structure and function. Physiologia Plantarum 110: 286-292.

23. Matsumura H, Reich S, Ito A, Saitoh H, Kamoun S, et al. (2003) Gene expression analysis of plant host-pathogen interactions by SuperSAGE. Proceedings of the National Academy of Sciences USA 100: 15718-15723.

24. Allen LJ, MacGregor KB, Koop RS, Bruce DH, Karner J, et al. (1999) The relationship between photosynthesis and a mastoparan-induced hypersensitive response in isolated mesophyll cells. Plant Physiology 119: 1233-1241.

25. Stern DS, Higgs DC, Yang J (1997) Transcription and translation in chloroplasts. Trends in Plant Science 2: 308-315.

26. Hess DF (2000) Light-dependent herbicides: An overview. Weed Sci 48: 160-170.

27. Abbink TEM, Peart JR, Mos TNM, Baulcombe DC, Bol JF, et al. (2002) Silencing of a gene encoding a protein component of the oxygen-evolving complex of photosystem II enhances virus replication in plants. Virology 295: 307-319.

28. Lincoln JE, Richael C, Overduin B, Smith K, Bostock R, et al. (2002) Expression of the antiapoptotic baculovirus p35 gene in tomato blocks programmed cell death and provides broad-spectrum resistance to disease. Proceedings of the National Academy of Sciences 99: 15217-15221.

29. Zhu J, Li M, Clough SJ (2015) Similarities and differences in global gene expression profiles between herbicide- and pathogen-induced PSII inhibition. Journal of Plant Biochemistry and Physiology (*submitted Sept 30, 2015; In press*).

30. Tao Y, Xie Z, Chen W, Glazebrook J, Chang HS, et al. (2003) Quantitative nature of Arabidopsis responses during compatible and incompatible interactions with the bacterial pathogen *Pseudomonas syringae*. The Plant Cell 15: 317-330.

31. Bors W, Heller W, Michel C, Saran M (1990) Flavonoids as antioxidants: determination of radical-scavenging efficiencies. Methods in Enzymology 186: 343-355.

32. Grace SC (2000) Energy dissipation and radical scavenging by the plant phenylpropanoid pathway. Philosophical Transactions of the Royal Society B: Biological Sciences 355: 1499-1510.